J. Coat. Technol. Res.
DOI 10.1007/s11998-015-9736-6

Facile synthesis of epoxy nanocomposite coatings using inorganic nanoparticles for enhanced thermo-mechanical properties: a comparative study

Rawaiz Khan, Muhammad Rizwan Azhar, Arfat Anis, Mohammad Asif Alam, M. Boumaza, Saeed M. Al-Zahrani

Abstract Epoxy-based nanocomposite coatings were formulated by incorporating various types of inorganic nanoparticles (NPs) (ZrO_2, ZnO, Fe_2O_3, and SiO_2). The effect of the incorporation of various NPs on the mechanical, thermal, and morphological properties of these epoxy coatings has been studied. A facile direct incorporation technique has been utilized for the dispersion of the NPs in the epoxy matrix via high-speed mechanical stirring and ultra-sonication using acetone as a solvent. The incorporation of these NPs augmented the mechanical and thermal properties of the epoxy coatings. The results revealed that the incorporation of small amount of these NPs improved the mechanical properties of the coating in all cases, with the SiO_2-reinforced sample being relatively better in both mechanical and thermal properties. The incorporation of Fe_2O_3 and ZnO resulted in a decrease in the thermal stability and glass transition temperature (T_g) of the coatings, while incorporation of SiO_2 and ZrO_2 increased the thermal stability as well as T_g of the coatings. A notable increase of 71% in hardness together with 26% increase in the elastic modulus of the epoxy coating was observed with the incorporation of 2 wt% SiO_2 NPs.

Keywords Epoxy, Reinforcement, Facile, Nanocomposite, Incorporation, Nanoindentation

R. Khan (✉), A. Anis, M. Boumaza, S. M. Al-Zahrani
Chemical Engineering Department, King Saud University, P.O. Box 800, Riyadh 11421, Saudi Arabia
e-mail: krawaiz@ksu.edu.sa

R. Khan, M. A. Alam, S. M. Al-Zahrani
Center of Excellence for Research in Engineering Materials (CEREM), Advanced Manufacturing Institute, King Saud University, P.O. Box 800, Riyadh 11421, Saudi Arabia

M. R. Azhar
Chemical Engineering Department, Curtin University, Bentley, WA, Australia

A. Anis, S. M. Al-Zahrani
SABIC Polymer Research Center (SPRC), King Saud University, P.O. Box 800, Riyadh 11421, Saudi Arabia

Introduction

Epoxy resin is a thermosetting polymer having excellent adhesion, chemical resistance, and electrical insulation properties. However, there are some limitations associated with the epoxy resins such as low thermal resistance and inability to form them into thin layers with ease because of their high viscosity. There is an increasing demand to synthesize thermally stable and easy-to-fabricate coatings, particularly for the modern electronic and electrical industry. The incorporation of inorganic nanoparticles (NPs) in the epoxy matrix can help improve its thermal, mechanical, electrical, and corrosion properties.[1–4] The properties of the organic–inorganic nano-composites are affected by several factors including type, size, shape, aspect ratio, and dispersion of the NPs in the polymer matrix.[5–12] Generally, there are three methods by which NPs are added and dispersed in the polymer matrix: (I) direct mixing of polymer and NPs, (II) in situ polymerization in the presence of NPs, and (III) simultaneous in situ polymerization and NP synthesis. The selection of incorporation method depends on several factors such as viscosity of the polymer, surface chemistry of the NPs, and the ratio of NPs/polymer. However, direct incorporation of NPs in the resin matrix is easier compared to the ''In situ polymerization in presence of NPs,'' and ''Simultaneous in situ polymerization and NPs synthesis.'' Moreover, in the case of in situ polymerization in the presence of NPs, pre-treatment of NPs is essential to modify the surface to avoid settling of the NPs. Similarly, in ''Simultaneous in situ

Published online: 08 September 2015

polymerization and NPs synthesis,'' more steps are involved to fabricate the coatings, along with complex chemistry involved in it.[13] Thermal stability is one of the most crucial properties for polymeric material, as it ultimately governs the mechanical properties, durability, spectral stability, shelf life, and life cycle of the polymers.[14–17] Once the degradation begins, the above-mentioned properties gradually deteriorate. However, the incorporation of inorganic NPs in polymers results in somewhat improved thermal resistance of the host polymer.[18,19] Moreover, organic–inorganic nanocomposite materials result in high-performance materials because they combine the advantages of inorganic materials (rigidity and high stability) and organic polymers (flexibility, dielectric, ductility, and processability) for various applications. From among several types of composite materials, epoxy nano-composites (ENCs) find a wide range of applications such as adhesives and protective coatings, in electrical, electronic, and aerospace industries. These types of nanocomposites fulfill both thermal and mechanical properties which are of prime importance for most of its applications. Epoxy resin systems that can be cured at room temperature are more favorable for incorporation of NPs.[20,21] The system based on the reaction of the di-functional epoxy monomer diglycidyl ether of bisphenol-A (DGEBA), with aliphatic amines, is one such example.

The addition of hard particles into polymers to improve their physical and mechanical properties is very common. These are generally ceramic particles such as SiO_2, ZnO, TiO_2, $CaCO_3$, etc.[21] Among them SiO_2 is the most used and studied particle.[22–25] In the present study, DGEBA and polyaminoamide adduct (R41) coating system is modified with the direct incorporation of different types of inorganic NPs. These NPs have been used by other researchers individually in different wt% in order to modify epoxy coating system in terms of thermal, mechanical, and corrosion properties.[6,10,11,16] However the focus of the current study is to have a comparative analysis of the effect of these NPs on thermal, mechanical, and morphological properties of the cured coatings. The addition of different types of filler into poly acrylic coating revealed that a small percentage of nano-alumina particles markedly improve the scratch and hardness properties of the coating.[26] Another comparative study on epoxy nanocomposite reported that epoxy coating modified with SiO_2 NPs showed a significantly enhanced Young's modulus of ~2.5 GPa.[27] Spirkova et al. studied the influence of nano-additives on surface, permeability, and mechanical properties of self-organized organic–inorganic nanocomposite coatings. The results revealed that colloid silica showed a pronounced effect on the final product crosslink density: silica bonded chemically to the matrix and increased the modulus in rubber state nearly three times.[28] Ramezanzadeh et al.[29] revealed that homogeneous dispersion and good combination of viscoelastic properties can be achieved at lower wt% of ZnO NPs (2 wt% and 3.5%), while higher wt% of these NPs causes agglomeration, particle aggregation, and reduction in T_g and crosslink density. The quantity of NPs is an important concern. High quantities of NPs not only increase the cost of the material and process, but also may result in agglomeration of the NPs, giving rise to undesirable properties.[30] Epoxy composite containing submicron TiO_2 particles treated with Al_2O_3–ZrO_2 develops higher tensile and flexural strength but lower elongation and ductility than those containing TiO_2 surface treated with Al_2O_3–SiO_2. This is attributed to the inferior adhesion of the Al_2O_3–ZrO_2-treated particles with the matrix.[31] Based on some previous studies[29,32–34] and prior experimental work, a fixed quantity (2 wt%) of ZrO_2, ZnO, Fe_2O_3, and SiO_2 NPs has been dispersed in epoxy matrix to avoid agglomeration and achieve good dispersion of the NPs. This study demonstrates the effect of these NPs on thermo-mechanical properties of the epoxy/polyamide system.

Experimental

Materials

Epoxy resin (EPON 1001-K-65) was obtained from Hexion Chemicals (USA); it has epoxide equivalent weight of 450–550 g/equiv. and Brookfield viscosity of 1500–4500 cP at 25°C. Polyaminoamide adduct R41 was obtained from Huntsman Advanced Materials. Acetone (Merck, 99%) has been used as a solvent. ZrO_2, ZnO, Fe_2O_3, and SiO_2 of same size, i.e., 50 ± 5 nm, were purchased from Sigma Aldrich. Steel panels and glass panels were purchased from the local market. The composition for different types of nanocomposite formulations is given in Table 1. The steel panels were thoroughly cleaned with acetone to remove grease and other dust particles. Similarly, the glass substrates were also well cleaned with the help of acetone and were allowed to dry for some time.

Sample preparation

Epoxy matrix was diluted with acetone to facilitate the dispersion of the NPs. The weight ratio of the hardener to the resin was 1:4. The mixing was carried out for 1 h at 3000 rpm using a high-speed mechanical stirrer (DispersMaster, Sheen Instruments. Ltd, UK). After mechanical mixing, the mixture was subjected to sonication at 50°C for 90 min. After partial removal of the solvent, hardener was added to the mixture and stirred mechanically at 600 RPM for 30 min. The solution was allowed to stabilize for 10 min. The application viscosity was controlled in the range from 4.5 to 5 poise.

The synthesized slurry was directly applied to steel and glass panels using a four-sided bird applicator

Table 1: Neat epoxy and nanoparticle-reinforced nanocomposite epoxy coating composition

Sample code	Resin 1001 (wt%)	Nanopowder (wt%)		Acetone (ml)	Silane (%)	Air releasing agent (%)	Hardener (wt%)
EP	80.67	–	0	25	2	0.5	19.33
EPZR		ZrO_2	2				
EPZN		ZnO	2				
EPFE		Fe_2O_3	2				
EPSI		SiO_2	2				

(80 mm width, gap sizes 30/60/90/120 μm, Sheen Instruments. Ltd, UK) with 90 μm gap size. The coated samples were ensured to have a uniform wet film thickness, and kept on a smooth surface in a dust-free environment. The curing and crosslinking process of the wet film took about 5 days to complete at ambient temperature.

Characterization

Fourier transform infrared spectroscopy (FTIR) spectra were recorded for the fabricated coatings on a Thermo-Scientific (Nicolet iN10) infrared spectrophotometer equipped with a liquid nitrogen-cooled mercury–cadmium–telluride detector. The surface morphology of the coatings was determined using field emission scanning electron microscope (FESEM) from JEOL (JSM7600F). The microscope was operated at 5 kV with a working distance of 4.5 mm. X-ray diffractometer from Bruker (D8 DISCOVER) has been used to study XRD patterns at operating voltage and current of 20 kV and 5 mA, respectively. The parameters for the XRD study are kept the same to identify the incorporation of the NPs. The step size and dwell time for 2θ values (in the range of 10°–80°) were maintained at 0.2° and 3 s, respectively.

Modulus and hardness of the coating samples were studied using standard nano-indentation testing. The tests were performed using a Nano test 600 nano-mechanical testing system (Micro Materials, UK) on the prepared samples. The nano-indenter monitors and records the load and displacement of the indenter with a force resolution of ~100 nN and a displacement resolution of ~0.1 nm. Tests were performed inside the nano-indenter's thermally insulated environmental chamber, at a room temperature of 25 ± 0.5°C and a relative humidity of 45 ± 2% on unreinforced and reinforced coating samples. A constant load of 250 mN was used with a loading/unloading rate of 10 mN/min. The indentation test parameters were held constant to compare the results obtained for the unreinforced epoxy matrix and the ENCs. The samples were mounted on an aluminum stub and indented to ~250 mN. The unloading load–displacement curves were analyzed to determine hardness and modulus using Oliver–Pharr theory[35] with the projected area imaged under SEM. Nano-indentation short-term creep tests were performed at 100 mN load with a dwell period of 30 s for all compositions.

The pendulum hardness (ASTM D 4366) was measured with respect to pendulum oscillation times on the coatings from 6° to 3° at 23 ± 1°C and 50 ± 2% relative humidity. A Konig pendulum hardness tester (Sheen Instruments Ltd, UK) was used to monitor the surface hardness of the cured film after curing at room temperature. Automatic scratch tester (REF705, Sheen Instruments Ltd, UK) was used to check the scratch resistance of the coating samples by applying a scratch probe with different available loadings. The load was increased until the probe damaged the coating surface.

Impact strength was measured by dropping a standard weight from a distance, so as to strike an indenter that damages the coating and the substrate. The damage can either be an intrusion or an extrusion. The dropping weight distance is gradually increased to determine the failure point. The failure occurs in films mostly as cracks, which can be visualized using a magnifier. The height at which the film's crack is denoted as the failure points in force-inch-pound (f-in-lb). The apparatus used was BYK-Gardner impact tester from sheen instruments, UK (Model: IG-1120) following ASTM D 2794. Differential scanning calorimetry (DSC) experiments were performed on a TA Instrument DSC 2920 simultaneously to measure T_g and other thermal properties. The instrument was calibrated according to the manufacturer's procedure, using indium as the standard reference material. Samples were weighed (approximately 15–20 mg) and loaded into the DSC cell. T_g was determined using the midpoint temperature, which is the point on the thermal curve corresponding to one half of the heat flow difference between the extrapolated onset point of transition and the end inflection change.[36] The tests were performed at a heating rate of 10°C/min from room temperature to 600°C in nitrogen atmosphere (100 ml/min).

Results and discussion

Microstructure characterization

Field emission scanning electron microscopy was performed to investigate the dispersion of NPs in epoxy matrix after sputtering a thin gold layer on the

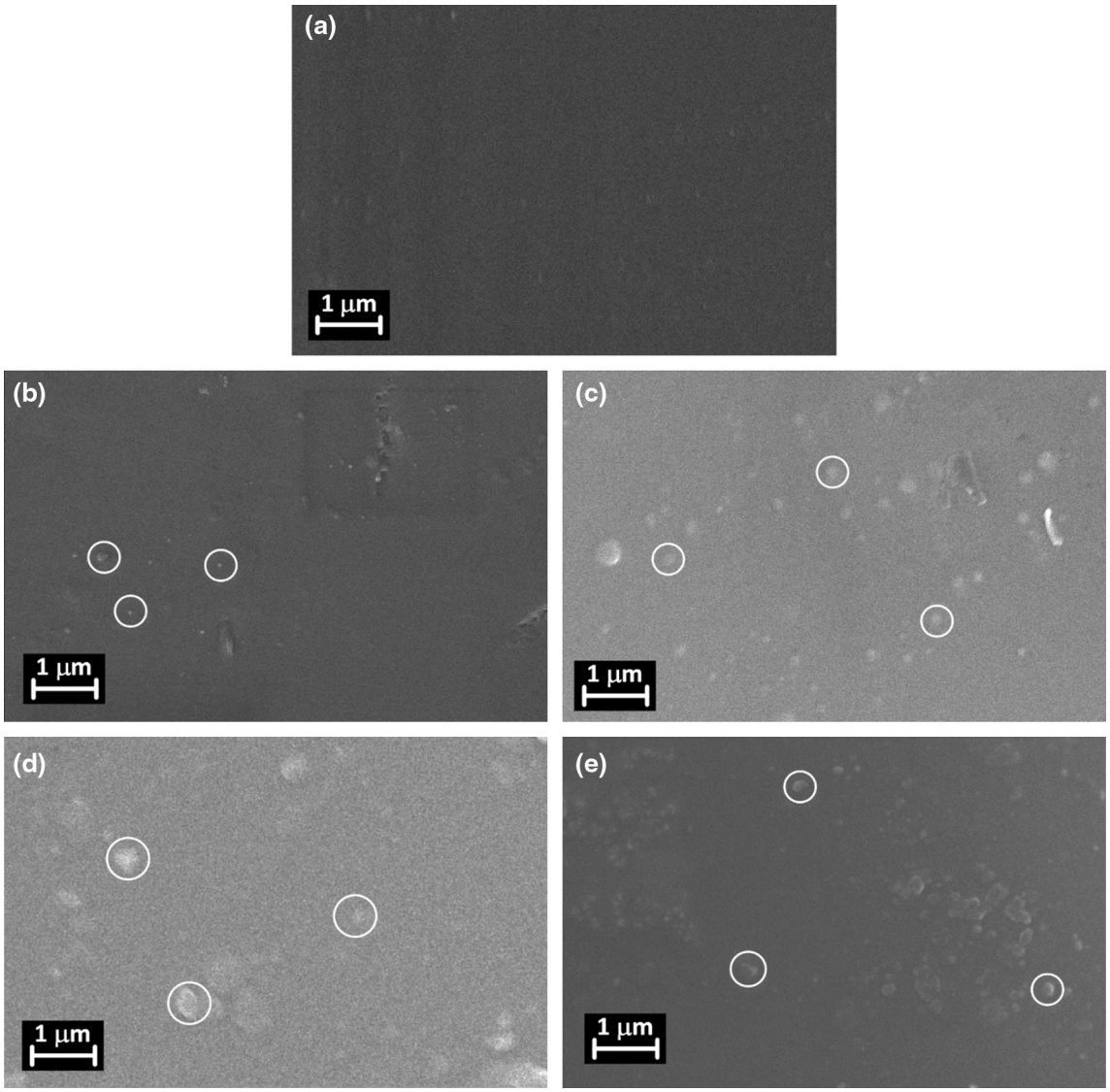

Fig. 1: SEM micrographs of pristine and reinforced coating: (a) EP, (b) EPSI, (c) EPFE, (d) EPZN, and (e) EPZR

top surface. Typical FESEM micrographs for the pristine and reinforced coating samples are shown in Fig. 1. The dispersion of NPs at high loadings in the epoxy matrix is a challenging process. Therefore, low wt% of NPs is used at reduced viscosity in the presence of a solvent, via mechanical stirring and sonication. However, the high tendency of NPs to agglomeration caused partial agglomeration in the matrix except EPSI which has comparatively better dispersion and uniform distribution of NPs, as given in FESEM micrographs. The particles are partially aggregated which shows a poor dispersion of NPs. Ramezanzadeh et al. [32–34] studied the effect of ZnO NPs on the thermal, mechanical, viscoelastic, and corrosion properties of epoxy–polyamide coatings. They incorporated ZnO NPs in the range of 2 to 6.5 wt% and reported that higher NP loadings (5 and 6.5 wt%) caused agglomeration and particle aggregation.

Fourier transform infrared spectroscopy and X-ray diffraction analysis

The spectra of the pristine DGEBA epoxy and ENCs DGEBA- R41-X (where X is the NPs added) coatings are shown in Fig. 2. The spectra were collected in the range of 500 to 4000 cm^{-1} to study the spectra from the coated surfaces. The chemical structure of DGEBA molecule contains a variety of organic groups such as aromatic rings, –CH3, ≡ C–O–C ≡ , etc.[37] R41 has a heterocyclic amine chemical structure that contains multi-functional groups such as –N ≡ N–, –NH, –OH, =C=O, etc. The FTIR spectra regions correspond to CH band (2800–2962 cm^{-1}), epoxide ring (~825 cm^{-1}), NH band of primary amines (1580–1650 cm^{-1}), OH groups (~3400 cm^{-1}), CN band (1000–1100 cm^{-1}), and etheric bands (~1230 cm^{-1}).[38] The broad peak at 3200–3500 cm^{-1} shows the O–H bonds of aromatic ring

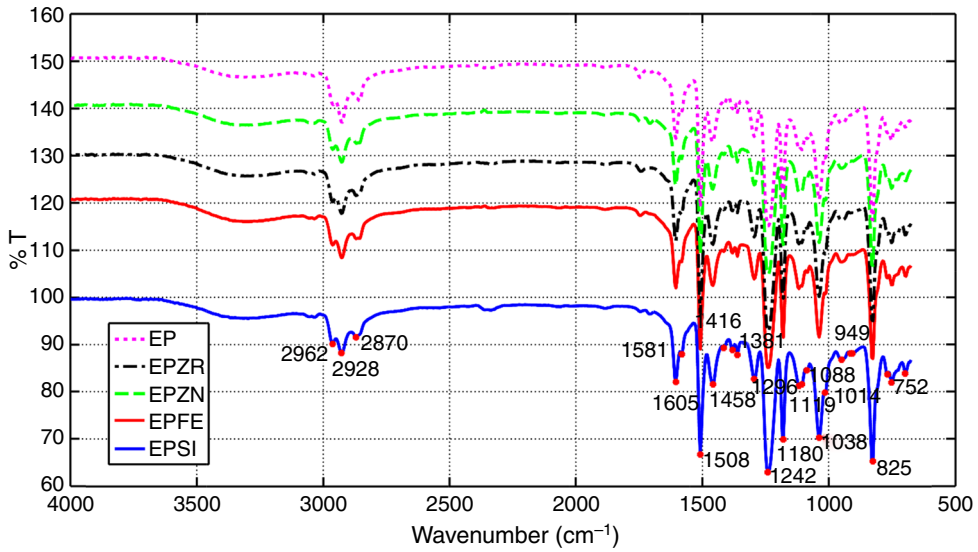

Fig. 2: FTIR spectra for pristine epoxy and NP-reinforced coatings

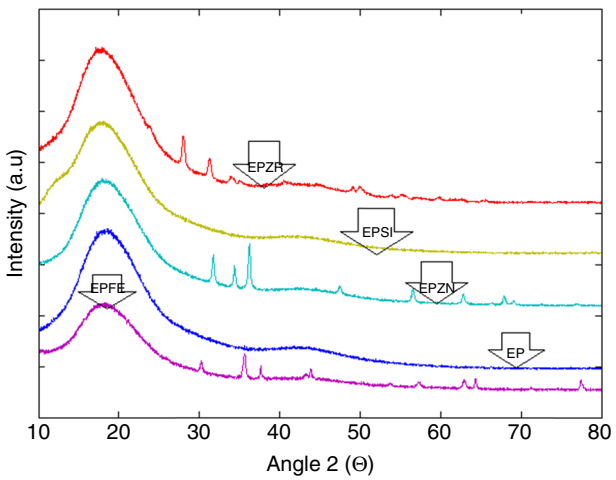

Fig. 3: XRD pattern for pristine and NP-reinforced coatings

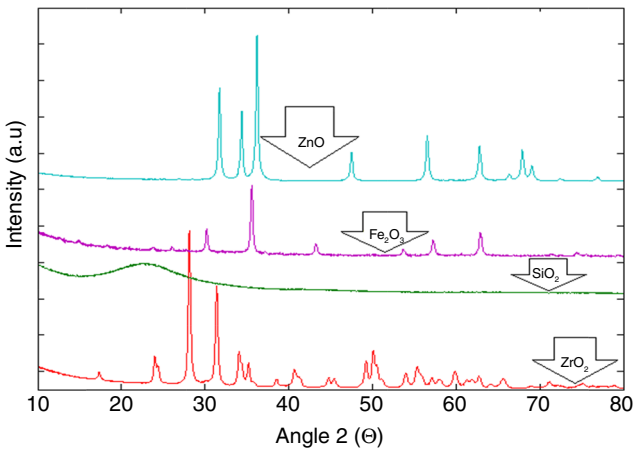

Fig. 4: XRD spectra of the pure nanoparticles

stretching and N–H stretching which show the interaction of epoxy and hardener, while peaks at around 2900 cm^{-1} (2962, 2924, and 2966 cm^{-1}) are attributed to C–H of DGEBA. These peaks are present in all compositions which confirms the presence of DGEBA structure in the ENC coatings.[39] The peaks at 1581 and 1605 cm^{-1} confirm the N–H band of the primary amine group, which is of the same intensity in all compositions, indicating hardener–epoxy interaction. At 1509 cm^{-1}, a strong peak indicates asymmetric N–O stretching, which is an indication of nitro compounds. The peaks at 1458 cm^{-1} and 1238–1242 cm^{-1} show the C–C and C–O stretching in all the compositions. The strong peak at 827 cm^{-1} indicates C–H in the aromatic ring. The peak in the range of 900–1190 cm^{-1} suggests asymmetric stretching of the epoxide ring,[40] which can be attributed to the interaction of the amine with epoxide or oxirane group. The major contribution is the bond stretching and bond vibration due to the crosslinking of amino groups of the hardener. Moreover, the NPs act as a catalyst and lower the activation energy to facilitate the bonding between the epoxy and the hardener.[34,41] XRD patterns for the ENC coatings and the pristine NPs are shown in Figs. 3 and 4, respectively. A broad peak in the range of 15°–25° confirms the amorphous nature of the epoxy coatings.[42] In the case of the composite coatings, the trends are almost the same regarding the epoxy peaks, while subsequent peaks of the NPs also appear at their respective locations. The intensity of the NPs peaks is quite less in ENCs, as the concentration of the NPs is very low (2 wt%) in the coating matrix; this is also confirmed by the EDS pattern. The nature of the NPs is crystalline except for SiO_2 NPs which shows an amorphous nature. All the NPs, other than SiO_2, are polycrystalline as indicated by their peaks at different locations.

Mechanical properties

Nano-indentation was used to study the hardness and modulus property of the neat epoxy and ENC coatings. A set of different raw loading/unloading curves is shown in Fig. 5. The indentation depths at the peak load ranges from around 8.9 μm (EPSI) to 11 μm (EP). Least indentation depths are observed for the EPSI sample. Figure 5 elucidates the set of loading–unloading–displacement curves of indentations made at a peak indentation load of 250 mN. Since no steps or discontinuities were observed on the loading curves, it indicates no crack formation during the course of indentation. The SEM images of the indentations are given in Fig. 6 which confirms the absence of cracking on the surface.

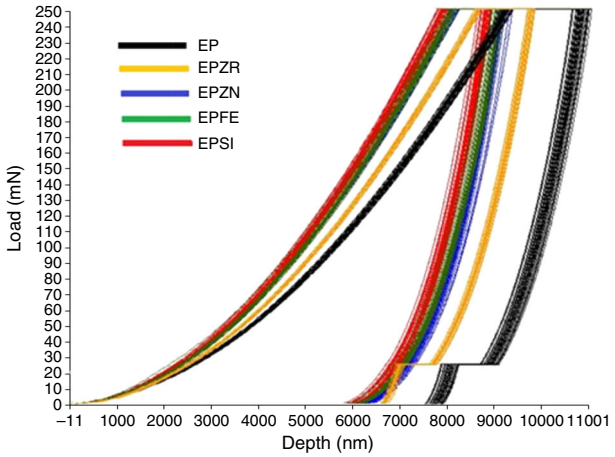

Fig. 5: Combined loading/unloading indentation curves for pristine and reinforced epoxy coating

Figure 7 shows a graphical representation of hardness and modulus for pure and nanocomposite epoxy coating samples. Modulus is obtained using the Oliver–Pharr theory and the unloading portion of the nano-indentation curve to obtain the reduced modulus (E_r). Sattari et al.[43] used the same method for calculation of elastic modulus and hardness as given in equations (1), (2), and (3).

$$\frac{1}{E_r} = \frac{1-\nu^2}{E} + \frac{1-\nu_i^2}{E_i} \tag{1}$$

$$E = \frac{E_i E_r (1-\nu^2)}{E_i - E_r (1-\nu_i^2)} \tag{2}$$

$$H = \frac{F_{max}}{A}, \tag{3}$$

where E is the modulus of the sample, ν is the Poisson's ratio normal to loading of the sample, E_i is the indenter modulus, ν_i is the indenter Poisson's ration normal to loading, H is the hardness, F_{max} is the maximum normal load, and A is the projected contact area at the maximum load. The indenter is diamond with E_i = 1141 GPa and ν_i = 0.07; ν is taken as 0.3 due to the matrix (polymer)-dominated response in this direction.[44] The specimens Poisson's ratio is expected to change as a function of wt% of NPs, but that effect is not considered in the data reduction herein. The results confirm that the addition of small amount of the NPs to epoxy matrix resulted in an increase in hardness and elastic modulus. It can also be seen from Fig. 5 that the EPSI has smaller depth value and indentation area, while having the relatively highest slope of unloading curve. Thus EPSI has relatively better mechanical properties with about a 71% and 26% increase in

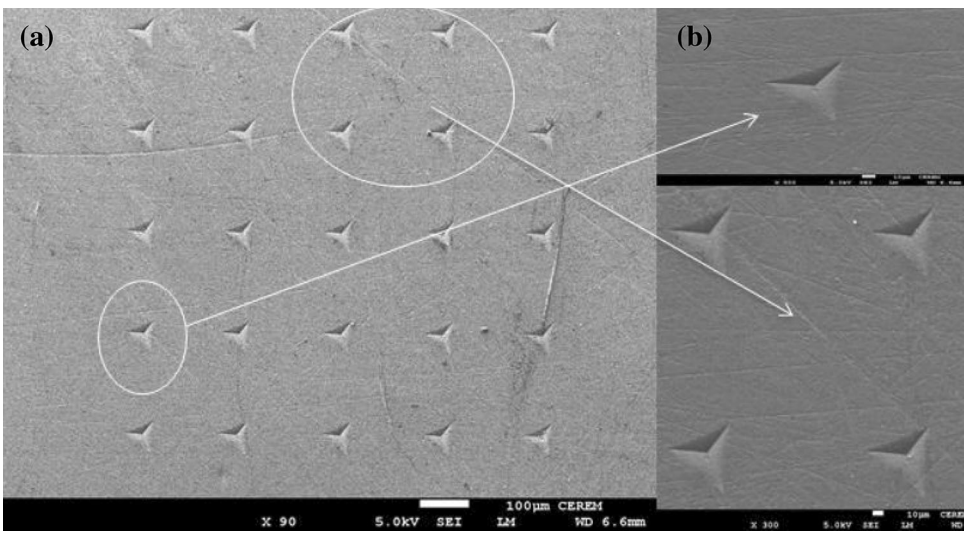

Fig. 6: SEM images of set of 25 indents at (a) low magnification and (b) high magnification

hardness and elastic modulus, respectively. The values for hardness are shown in Table 2. The value of the modulus increased due to the high modulus value of silica NPs $E = 70$ GPa.[45–47] Similar effects were noticed by Sattari et al.[43] by the addition of SiO_2 in a polymer matrix. EPZR showed relatively highest indentation depth and, consequently, the lowest hardness and modulus values. The reason could be the reduction in curing rate in the presence of ZrO_2 NPs, due to which the nanocomposite could not induce a higher crosslink density as compared to the other samples. EPZN and EPFE showed higher values of hardness and modulus compared to EPZR but lower than EPSI. This indicates a moderate crosslink density and better matrix-to-particle interaction as compared to EPZR. The addition of 2 wt% ZrO_2, ZnO, Fe_2O_3, and SiO_2 NPs causes a 28, 56, 61, and 71% increase in the hardness, whereas the modulus increased by 4, 25, 21, and 26%, respectively. Shi et al.[27] reported highest hardness and elastic modulus values of SiO_2 in comparison with neat and Fe_2O_3, Zn, and nanoclay composites which is in good agreement with our results. The finely smooth surface morphology of FESEM in Fig. 1b shows that SiO_2 NPs are compatible with the epoxy matrix. Therefore, SiO_2 NPs' addition serves to bridge more molecules in the interconnected matrix as compared to other NPs, leading to increased crosslinking density and forming highly compact, one-phase structure of the cured nanocomposite coating.

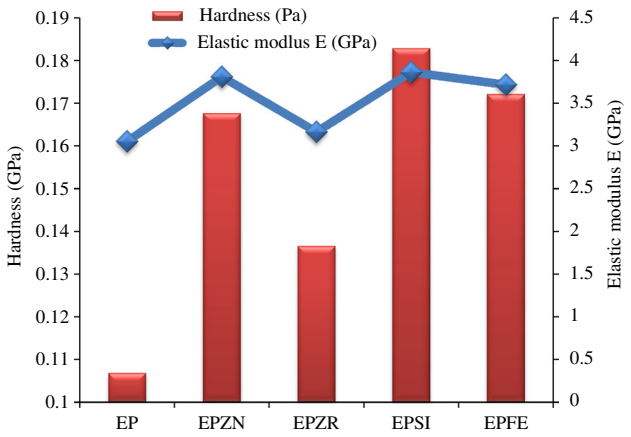

Fig. 7: Comparison of hardness and elastic modulus for neat and reinforced coating samples

The high filler/matrix interaction of SiO_2 may be attributed to amorphous nature and high specific surface area (≥450 m^2/g) of SiO_2, which make it more compatible with amorphous epoxy matrix. The lower mechanical properties of the other NPs can be attributed to their lower specific surface area and lower compatibility (due to crystalline phase) with amorphous epoxy matrix. Allahvardi et al.[36] incorporated 5 wt% of SiO_2 in epoxy matrix with hardener-to-resin ratio of 1:2 and reported the highest values of elastic modulus and hardness of 4 and 0.18 GPa, respectively. Zhang et al. predicted the formation of an interphase in silica nanoparticle-modified epoxies.[48] In the current study, higher values of both hardness and modulus were obtained by incorporation of 2 wt% of SiO_2 with a hardener-to-resin ratio of 1:4. The incorporation of the NPs enhanced the mechanical properties in terms of hardness and elastic modulus. These NPs possess strong interfacial adhesion with the matrix enhancing the crosslinking density of the cured epoxy. Moreover, they reduce the chain segmental movements, thereby preventing epoxy disaggregation during the curing process.[20,27]

Similarly, an increase in creep resistance and a decrease in creep deformation of the composite coating are observed in all the nanocomposite coatings. The reason could be reduction in chain mobility of epoxy by NPs, acting as sites, blocking the movement of epoxy chains when subjected to an external indentation force; hence, they restrict the viscous flow of the amorphous epoxy. Also a good load transfer between epoxy matrix and the filler may give rise to good creep resistance of the nanocomposite as a whole.[20] The inherent properties of the incorporated SiO_2, such as high aspect ratio and the large interfacial area, contribute significantly in enhancing the interface adhesion between the NPs and the epoxy matrix, thus resulting in high values of creep resistance.[49] From Fig. 8, it is clear that the results of the creep test are in agreement with those of nano-indentation hardness and modulus analysis, with EPSI showing the least deformation followed by EPZN. However, EPFE and EPZR showed lower creep deformation as compared to unreinforced sample (EP). It is well established from the literature that the addition of silica NPs improves the creep without adversely affecting the thermo-mechanical properties of the epoxy polymer.[45]

The results from nano-indentation and creep test were verified by the pendulum hardness of the cured

Table 2: Hardness, reduced modulus, and elastic modulus obtained from nano-indentation of pure and nanocomposite epoxy coatings

Sample code	Nanoparticles	wt%	Hardness (GPa)	Reduced modulus E_r (GPa)	Elastic modulus E (Gpa)
EP	0	0	0.11	3.34	3.05
EPZR	ZrO_2	2	0.14	3.46	3.16
EPZN	ZnO	2	0.17	4.17	3.81
EPFE	Fe_2O_3	2	0.17	4.07	3.71
EPSI	SiO_2	2	0.18	4.23	3.86

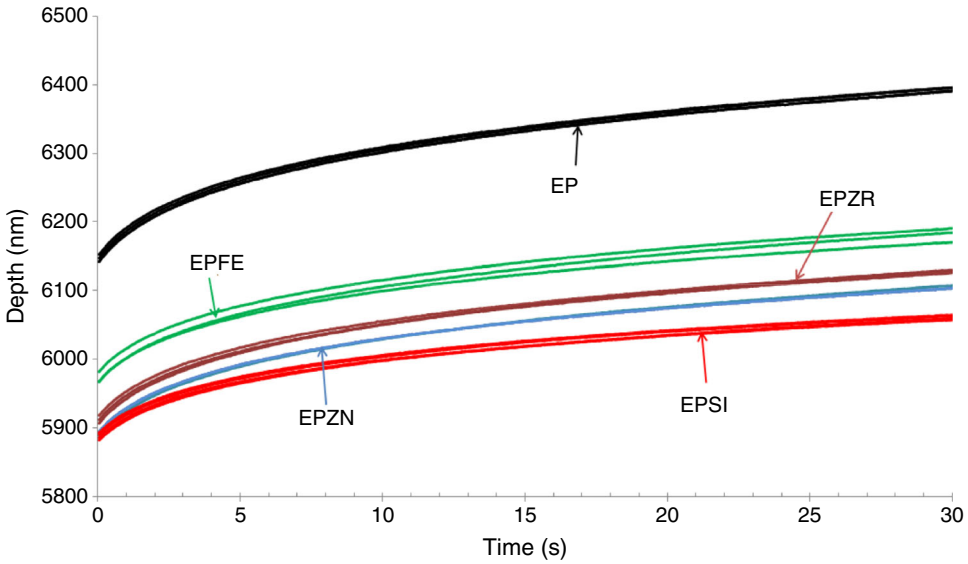

Fig. 8: Nano-indentation short-term creep deformation results

Table 3: Pendulum hardness for pure and nanocomposite epoxy coatings

Sample no.	EP	EPZR	EPZN	EPFE	EPSI
1	118	127	125	128	130
2	116	125	125	128	133
3	120	125	126	129	132
4	122	126	127	127	131
5	118	127	127	130	131
Average	118.8	126	126	128.4	131.4

Table 4: Comparison of impact and scratch resistance of pure and nanocomposite epoxy coatings

Sample code	Dry film thickness (μm)	Impact resistance lb/in^2	Scratch resistance (Kg)	Mandrel bend
EP	90–100	112	6	Pass
EPZR	90–100	128	8	Pass
EPZN	90–100	176	8.5	Pass
EPFE	90–100	120	7.5	Pass
EPSI	90–100	136	9	Pass

films coated on glass plates instead of steel substrate, having same coating thickness. The results for pendulum hardness are shown in Table 3. The pendulum hardness of the cured EPZN and EPZR films showed similar trends, while EPSI and EPFE films showed slightly higher values. The incorporation of all the NPs provides improvement in the pendulum hardness of the cured film in comparison to EP, with EPSI showing the highest values. The survival of such coatings is crucial under harsh mechanical conditions; hence the physico-mechanical properties of the composite coatings were tested by impact and scratch testing. The thickness of the coatings was 90–100 μm. It was noticed that all the composite coatings with 2 wt% loadings of the NPs increased and passed the impact test of 120 lb/in^2 as compared to the unreinforced coating which cracks at 112 lb/in^2. However, the impact value for EPZN remains the highest and showed 57% increase in the impact resistance. This can be attributed to some plasticizing effects from ZnO. Similarly, the scratch resistance for all the samples increased in all compositions, and EPSI was found to have the highest scratch load. The summary of the results is given in Table 4. A graphical representation of scratch and impact resistance for all compositions is shown in Fig. 9. The increasing trend in the scratch hardness values can be attributed to the improvement in the adhesion between composite coating and metal substrate. The higher

surface-to-volume ratio of SiO_2 results in better adhesion between the epoxy matrix and the metal substrate. Moreover, the higher degree of crosslinking of SiO_2 with DGEBA matrix leads to the formation of a dense and compact composite structure. One of the possible reasons can be the yielding of the matrix to decrease the local stress concentrations by the NPs.[50]

Thermal Properties

The glass transition temperature (T_g) of the pristine and reinforced coating samples was studied using DSC. The heat flow vs temperature diagram for all the ENC samples is shown in Fig. 10. It is evident from the obtained results as shown in Table 5 that T_g of EPSI and EPZR increased with the addition of 2 wt% of SiO_2 and ZrO_2 NPs, respectively. Allahverdi et al.[36] reported the T_g of 48.9°C for cured neat epoxy. However, the addition of 3 wt% of SiO_2 takes the T_g value up to 54.2°C. In the present study, a maximum T_g value of 59°C was obtained in the case of SiO_2. This increase in T_g can be attributed to the restricted mobility of the epoxy chains caused by the strong interactions between the NPs and the epoxy matrix.[51,52] The addition of 2 wt% of Fe_2O_3 and ZnO, however, slightly decreased the value of the glass transition temperature by imparting some plasticizing effect.

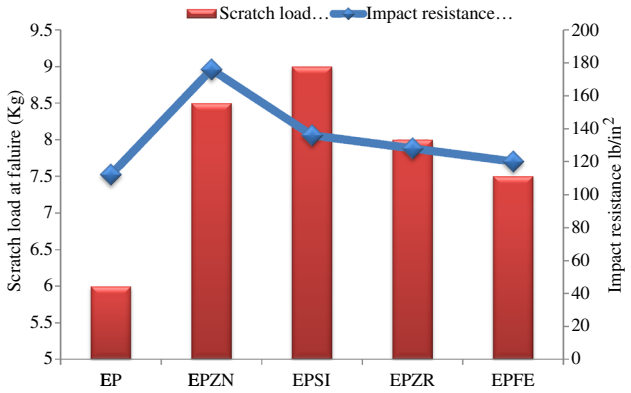

Fig. 9: Comparison of scratch and impact resistance

Table 5: DSC results for pure and nanocomposite epoxy coatings

Coating sample	T_g (°C)
EP	56.8
EPZR	58.0
EPZN	55.6
EPFE	55.0
EPSI	59.0

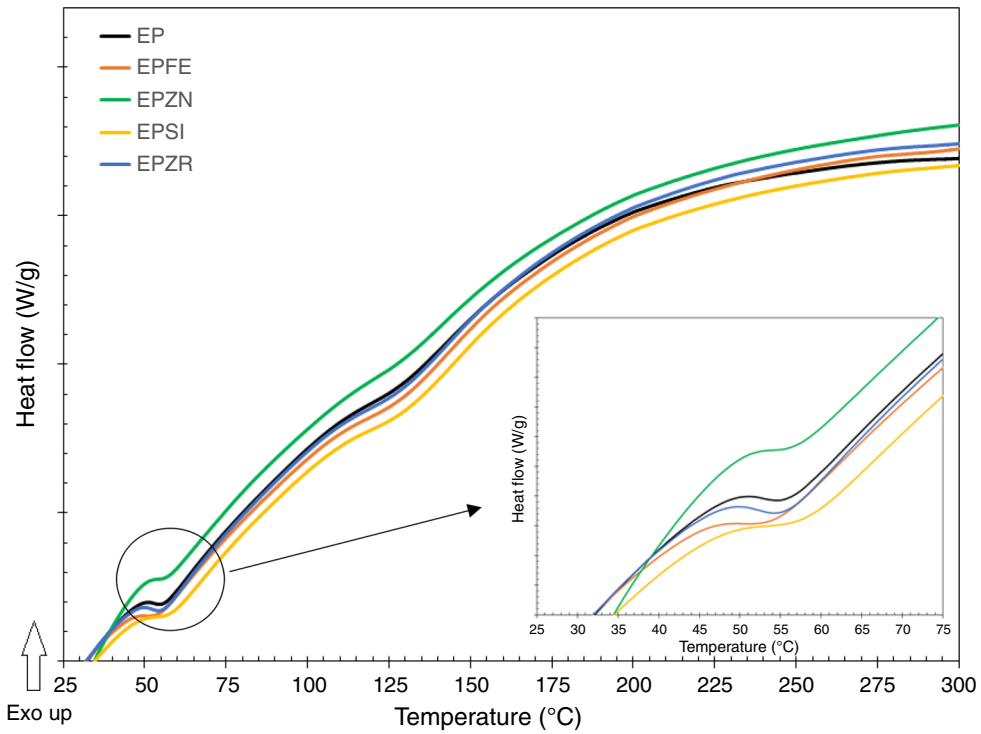

Fig. 10: DSC results for pristine and modified nanocomposite coating samples

Conclusion

A uniform morphology and good dispersion of the NPs in the epoxy matrix can be obtained using 2 wt% of the NPs. The addition of either ZnO, ZrO_2 or Fe_2O_3 or SiO_2 NPs increased the elastic modulus and hardness of ENC coatings. SiO_2 NPs show better interaction and adhesion with the epoxy matrix due to its amorphous nature and, thus, results in the best thermo-mechanical properties among the studied NPs. Incorporation of 2 wt% of SiO_2 in epoxy matrix gives higher values of hardness and elastic modulus of 0.18 and 4.2 GPa, respectively. Moreover, 2 wt% SiO_2 addition results in relatively better thermal stability of the nanocomposite coating in comparison to the other NPs. The glass transition temperature (T_g) for both SiO_2 and ZrO_2 is higher than for neat epoxy coating. SiO_2 nanocomposite showed the highest value of T_g as 59°C. The incorporation of both Fe_2O_3 and ZnO NPs showed reduction in the T_g of these ENCs.

Acknowledgment The authors gratefully acknowledge the financial support from the Research Center, College of Engineering, King Saud University.

References

1. El Saeed, AM, Fattah, MAE, Dardir, MM, ''Synthesis and Characterization of Titanium Oxide Nanotubes and Its Performance in Epoxy Nanocomposite Coating.'' *Prog. Org. Coat.*, **78** 83–89 (2015)
2. Wu, J, Ling, L, Ma, G, Wang, B, ''A Comparative Study of Grafting Steps on the Preparation and Properties of Modified Nanosilica for UV-Curable Coatings.'' *J. Coat. Technol. Res.*, **11** (5) 717–725 (2014)
3. Fletcher, A, Gupta, MC, Dudley, KL, Vedeler, E, ''Elastomer Foam Nanocomposites for Electromagnetic Dissipation and Shielding Applications.'' *Compos. Sci. Technol.*, **70** (6) 953–958 (2010)
4. El-Tantawy, F, Kamada, K, Ohnabe, H, ''In Situ Network Structure, Electrical and Thermal Properties of Conductive Epoxy Resin–Carbon Black Composites for Electrical Heater Applications.'' *Mater. Lett.*, **56** (1–2) 112–126 (2002)
5. Pervin, F, Zhou, Y, Rangari, VK, Jeelani, S, ''Testing and Evaluation on the Thermal and Mechanical Properties of Carbon Nano Fiber Reinforced SC-15 Epoxy.'' *Mater. Sci. Eng. A*, **405** (1–2) 246–253 (2005)
6. Adachi, T, Osaki, M, Araki, W, Kwon, S-C, ''Fracture Toughness of Nano- and Micro-Spherical Silica-Particle-Filled Epoxy Composites.'' *Acta Mater.*, **56** (9) 2101–2109 (2008)
7. Al-Turaif, HA, ''Effect of Nano TiO2 Particle Size on Mechanical Properties of Cured Epoxy Resin.'' *Prog. Org. Coat.*, **69** (3) 241–246 (2010)
8. Omrani, A, Simon, LC, Rostami, AA, ''The Effects of Alumina Nanoparticle on the Properties of an Epoxy Resin System.'' *Mater. Chem. Phys.*, **114** (1) 145–150 (2009)
9. Ahmadi, B, Kassiriha, M, Khodabakhshi, K, Mafi, ER, ''Effect of Nano Layered Silicates on Automotive Polyurethane Refinish Clearcoat.'' *Prog. Org. Coat.*, **60** (2) 99–104 (2007)
10. Wichmann, MHG, Cascione, M, Fiedler, B, Quaresimin, M, Schulte, K, ''Influence of Surface Treatment on Mechanical Behaviour of Fumed Silica/Epoxy Resin Nanocomposites.'' *Compos. Interfaces*, **13** (8–9) 699–715 (2006)
11. Chen, Q, Chasiotis, I, Chen, C, Roy, A, ''Nanoscale and Effective Mechanical Behavior and Fracture of Silica Nanocomposites.'' *Compo. Sci. Technol.*, **68** (15–16) 3137–3144 (2008)
12. Wang, H, Bai, Y, Liu, S, Wu, J, Wong, CP, ''Combined Effects of Silica Filler and Its Interface in Epoxy Resin.'' *Acta Mater.*, **50** (17) 4369–4377 (2002)
13. Schadler, LS, ''Polymer-based and Polymer-filled Nanocomposites.'' In: Ajayan, PM, Schadler, LS, Braun, PV (eds.) Nanocomposite Science and Technology, pp. 111–117. WILEY-VCH Verlag GmbH Co. KGaA, Weinheim (2003)
14. Cho, H-J, Jung, B-J, Cho, NS, Lee, J, Shim, H-K, ''Synthesis and Characterization of Thermally Stable Blue Light-Emitting Polyfluorenes Containing Siloxane Bridges.'' *Macromolecules*, **36** (18) 6704–6710 (2003)
15. Jin, J, Smith, DW, Topping, CM, Suresh, S, Chen, S, Foulger, SH, Rice, N, Nebo, J, Mojazza, BH, ''Synthesis and Characterization of Phenylphosphine Oxide Containing Perfluorocyclobutyl Aromatic Ether Polymers for Potential Space Applications.'' *Macromolecules*, **36** (24) 9000–9004 (2003)
16. Peng, Z, Kong, LX, Li, SD, Spiridonov, P, ''Poly(Vinyl Alcohol)/Silica Nanocomposites: Morphology and Thermal Degradation Kinetics.'' *J. Nanosci. Nanotechnol.*, **6** (12) 3934–3938 (2006)
17. Xia, R, Heliotis, G, Campoy-Quiles, M, Stavrinou, PN, Bradley, DDC, Vak, D, Kim, D-Y, ''Characterization of a High-Thermal-Stability Spiroanthracenefluorene-Based Blue-Light-Emitting Polymer Optical Gain Medium.'' *J. Appl. Phys.*, **98** (8) 083101 (2005)
18. Ji, X, Hampsey, JE, Hu, Q, He, J, Yang, Z, Lu, Y, ''Mesoporous Silica-Reinforced Polymer Nanocomposites.'' *Chem. Mater.*, **15** (19) 3656–3662 (2003)
19. Dalir, H, Farahani, RD, Nhim, V, Samson, B, Lévesque, M, Therriault, D, ''Preparation of Highly Exfoliated Polyester-Clay Nanocomposites: Process-Property Correlations.'' *Langmuir*, **28** (1) 791–803 (2012)
20. Vyazovkin, S, ''Modification of the Integral Isoconversional Method to Account for Variation in the Activation Energy.'' *J. Comput. Chem.*, **22** (2) 178–183 (2001)
21. Zhou, S, Wu, L, Sun, J, Shen, W, ''The Change of the Properties of Acrylic-Based Polyurethane Via Addition of Nano-Silica.'' *Prog. Org. Coat.*, **45** (1) 33–42 (2002)
22. Zhou, S, Wu, L, Shen, W, Gu, G, ''Study on the Morphology and Tribological Properties of Acrylic Based Polyurethane/Fumed Silica Composite Coatings.'' *J. Mater. Sci.*, **39** (5) 1593–1600 (2004)
23. Tahmassebi, N, Moradian, S, Ramezanzadeh, B, Khosravi, A, Behdad, S, ''Effect of Addition of Hydrophobic Nano Silica on Viscoelastic Properties and Scratch Resistance of an Acrylic/Melamine Automotive Clearcoat.'' *Tribol. Int.*, **43** (3) 685–693 (2010)
24. Wu, J, Xie, J, Ling, L, Ma, G, Wang, B, ''Surface Modification of Nanosilica with 3-Mercaptopropyl Trimethoxysilane and Investigation of its Effect on the Properties of UV Curable Coatings.'' *J. Coat. Technol. Res.*, **10** (6) 849–857 (2013)
25. Rostamzadeh, P, Mirabedini, SM, Esfandeh, M, ''APS-Silane Modification of Silica Nanoparticles: Effect Of Treatment's Variables on the Grafting Content and Colloidal Stability of the Nanoparticles.'' *J. Coat. Technol. Res.*, **11** (4) 651–660 (2014)

26. Sajjadi, SA, Avazkonandeh-Gharavol, MH, Zebarjad, SM, Mohammadtaheri, M, Abbasi, M, Mossaddegh, K, ''A Comparative Study on the Effect of Type of Reinforcement on the Scratch Behavior of a Polyacrylic-Based Nanocomposite Coating.'' *J. Coat. Technol. Res.*, **10** (2) 255–261 (2013)
27. Shi, X, Anh Nguyen, T, Suo, Z, Liu, Y, Avci, R, ''Effect of Nanoparticles on the Anticorrosion and Mechanical Properties of Epoxy Coating.'' *Surf. Coat. Technol.*, **204** 8 (2009)
28. Špírková, M, Strachota, A, Brožová, L, Brus, J, Urbanová, M, Baldrian, J, Šlouf, M, Bláhová, O, Duchek, P, ''The Influence of Nanoadditives on Surface, Permeability and Mechanical Properties Of Self-Organized Organic–Inorganic Nanocomposite Coatings.'' *J. Coat. Technol. Res.*, **7** (2) 219–228 (2010)
29. Ramezanzadeh, B, Attar, MM, ''Characterization of the Fracture Behavior and Viscoelastic Properties Of Epoxy-Polyamide Coating Reinforced with Nanometer And Micrometer Sized ZnO Particles.'' *Prog. Org. Coat.*, **71** (3) 242–249 (2011)
30. Huang, ZM, ''Tensile Strength of Fibrous Composites at Elevated Temperature.'' *Mater. Sci. Technol.*, **16** (1) 81–94 (2000)
31. Al-Turaif, H, ''Effect of TiO_2 Surface Treatment on the Mechanical Properties of Cured Epoxy Resin.'' *J. Coat. Technol. Res.*, **8** (6) 727–733 (2011)
32. Ramezanzadeh, B, Attar, MM, Farzam, M, ''Effect of ZnO Nanoparticles on the Thermal and Mechanical Properties of Epoxy-Based Nanocomposite.'' *J. Therm. Anal. Calorim.*, **103** (2) 731–739 (2011)
33. Ramezanzadeh, B, Attar, MM, ''Studying the Corrosion Resistance and Hydrolytic Degradation of an Epoxy Coating Containing ZnO Nanoparticles.'' *Mater. Chem. Phys.*, **130** (3) 1208–1219 (2011)
34. Ramezanzadeh, B, Attar, MM, Farzam, M, ''A Study on the Anticorrosion Performance of the Epoxy–Polyamide Nanocomposites Containing ZnO Nanoparticles.'' *Prog. Org. Coat.*, **72** (3) 410–422 (2011)
35. Oliver, WC, Pharr, GM, ''An Improved Technique for Determining Hardness and Elastic Modulus Using Load and Displacement Sensing Indentation Experiments.'' *J. Mater. Res.*, **7** (06) 1564–1583 (1992)
36. Allahverdi, A, Ehsani, M, Janpour, H, Ahmadi, S, ''The Effect of Nanosilica on Mechanical, Thermal and Morphological Properties of Epoxy Coating.'' *Prog. Org. Coat.*, **75** (4) 543–548 (2012)
37. Socrates, G, *Infrared and Raman Characteristic Group Frequencies: Tables and Charts*, 3rd ed., p. 366. Wiley, Chichester (2004)
38. Matin, E, Attar, MM, Ramezanzadeh, B, ''Investigation Of Corrosion Protection Properties of an Epoxy Nanocomposite Loaded with Polysiloxane Surface Modified Nanosilica Particles on the Steel Substrate.'' *Prog. Org. Coat.*, **78** 395–403 (2015)
39. Ramírez, C, Rico, M, Torres, A, Barral, L, López, J, Montero, B, ''Epoxy/POSS Organic–Inorganic Hybrids: ATR-FTIR and DSC Studies.'' *Eur. Polymer J.*, **44** (10) 3035–3045 (2008)
40. Jaya Vinse Ruban, Y, Ginil Mon, S, Vetha Roy, D, ''Mechanical and Thermal Studies of Unsaturated Polyester-Toughened Epoxy Composites Filled with Amine-Functionalized Nanosilica.'' *Appl. Nanosci.*, **3** (1) 7–12 (2012)
41. Ghaemy, M, Bazzar, M, Mighani, H, ''Effect of Nanosilica on the Kinetics of Cure Reaction and Thermal Degradation of Epoxy Resin.'' *Chin. J. Polym. Sci.*, **29** (2) 141–148 (2011)
42. Rong, Z, Sun, W, Xiao, H, Jiang, G, ''Effects of Nano-SiO_2 Particles on the Mechanical and Microstructural Properties of Ultra-High Performance Cementitious Composites.'' *Cement Concr. Compos.*, **56** 25–31 (2015)
43. Sattari, M, Naimi-Jamal, MR, Khavandi, A, ''Interphase Evaluation and Nano-Mechanical Responses of UHMWPE/SCF/Nano-SiO_2 Hybrid Composites.'' *Polym. Test.*, **38** 26–34 (2014)
44. Garcia, EJ, Saito, DS, Megalini, L, Hart, AJ, de Villoria, RG, Wardle, BL, ''Fabrication and Multifunctional Properties of High Volume Fraction Aligned Carbon Nanotube Thermoset Composites.'' *J. Nano Syst. Technol.*, **1** (1) 1–11 (2009)
45. Bray, DJ, Dittanet, P, Guild, FJ, Kinloch, AJ, Masania, K, Pearson, RA, Taylor, AC, ''The Modelling of the Toughening of Epoxy Polymers Via Silica Nanoparticles: The Effects of Volume Fraction and Particle Size.'' *Polymer*, **54** (26) 7022–7032 (2013)
46. Hsieh, TH, Kinloch, AJ, Masania, K, Taylor, AC, Sprenger, S, ''The Mechanisms and Mechanics of the Toughening of Epoxy Polymers Modified with Silica Nanoparticles.'' *Polymer*, **51** (26) 6284–6294 (2010)
47. Tetard, L, Passian, A, Lynch, RM, Voy, BH, Shekhawat, G, Dravid, V, Thundat, T, ''Elastic Phase Response of Silica Nanoparticles Buried in Soft Matter.'' *Appl. Phys. Lett.*, **93** (13) 133113 (2008)
48. Zhang, H, Zhang, Z, Friedrich, K, Eger, C, ''Property Improvements of In Situ Epoxy Nanocomposites with Reduced Interparticle Distance at High Nanosilica Content.'' *Acta Mater.*, **54** (7) 1833–1842 (2006)
49. Yang, J, Zhang, Z, Friedrich, K, Schlarb, AK, ''Creep Resistant Polymer Nanocomposites Reinforced with Multiwalled Carbon Nanotubes.'' *Macromol. Rapid Commun.*, **28** (8) 955–961 (2007)
50. Chonkaew, W, Sombatsompop, N, Brostow, W, ''High Impact Strength and Low Wear of Epoxy Modified by a Combination of Liquid Carboxyl Terminated Poly(Butadiene-Co-Acrylonitrile) Rubber and Organoclay.'' *Eur. Polymer J.*, **49** (6) 1461–1470 (2013)
51. Stojanovic, D, Orlovic, A, Markovic, S, Radmilovic, V, Uskokovic, P, Aleksic, R, ''Nanosilica/PMMA Composites Obtained by the Modification of Silica Nanoparticles in a Supercritical Carbon Dioxide–Ethanol Mixture.'' *J. Mater. Sci.*, **44** (23) 6223–6232 (2009)
52. Isik, I, Yilmazer, U, Bayram, G, ''Impact Modified Epoxy/Montmorillonite Nanocomposites: Synthesis and Characterization.'' *Polymer*, **44** (20) 6371–6377 (2003)